

Advances in Functional Testing With SFF Parts

Alan J. Dutson, Kristin L. Wood, Joseph J. Beaman, Richard H. Crawford

Department of Mechanical Engineering
The University of Texas at Austin

Abstract

Functional testing of SFF parts represents an exciting area of research in solid freeform fabrication. One approach to functional testing is to use similitude techniques to correlate the behavior of an SFF model and a product. Previous research at UT Austin has resulted in development of an empirical similitude technique to correlate the behavior of parts of dissimilar materials and geometry. Advances in the empirical similitude technique are presented in this paper. Sources of coupling between material and geometry characteristics that produce errors in the current empirical similitude technique are outlined. A modified approach that corrects for such errors is presented. Numerical examples are used to illustrate both the current and the advanced empirical similitude methods.

I. Introduction

The product development process can be abstracted into three broad categories: design; evaluation; and fabrication (see Figure 1). The design and evaluation activities are iterated until a satisfactory design (one that meets customer needs) is achieved. If the design and evaluation activities have been performed properly, then the product fabrication stage can be carried out without further changes to the design. If, however, the design has not been properly evaluated and refined, then product fabrication will yield unexpected results that can only be corrected through design changes. Since late design changes are extremely expensive and difficult to implement, it is essential that a design be thoroughly evaluated and refined before fabrication begins.

Prototypes are a powerful and commonly used means of evaluating product designs. Prototypes can be either physical or virtual in nature. *Virtual prototypes* include computer models, simulations, virtual reality, etc. Physical prototypes can either be *traditional prototypes*, which are created through typical manufacturing processes and manual construction, or *rapid prototypes*, which are created through solid freeform fabrication techniques.

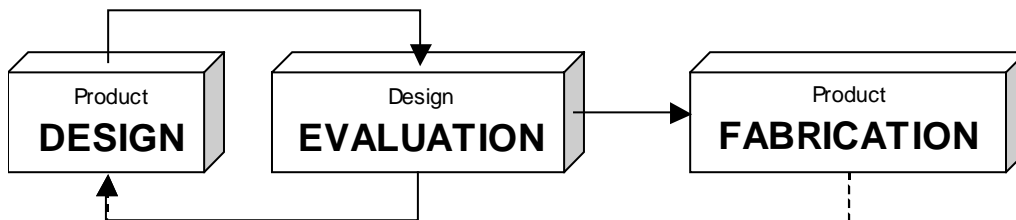


Figure 1. Abstraction of Product Development Process.

Improvements in computer equipment and software tools have produced a trend in many industries of using more virtual prototypes and fewer physical prototypes. The primary reason for this trend is found in the relative benefits of virtual prototypes, which typically include low costs and the ability to quickly evaluate changes in product designs. Significant reductions in development time and costs have been attributed to the use of virtual prototyping techniques. However, virtual prototypes have not entirely replaced physical prototypes in most development processes. Reasons for the continued use of physical prototypes include the following:

- Physical prototypes are often better suited for certain types of product evaluations, such as ergonomics, proportions, customer feedback, etc.
- Physical prototypes capture physical phenomena that may have been overlooked in the virtual models.
- Testing of physical prototypes can be a valuable aid in the verification / refinement process for virtual models.

The third item listed above indicates that physical and virtual prototypes can work as *complements* to each other in improving the design process. The goal of our research is to improve the way in which physical prototypes are used in verifying and refining virtual models. The specific objective of this research is to reduce the time required to verify virtual models by performing functional testing on rapid prototypes instead of on traditional prototypes. Replacing traditional prototypes with rapid prototypes can result in significant reductions in product development cycle times.

Functional testing has traditionally not been performed with rapid prototypes since material properties and part sizes that are available from RP technologies are rarely the same as those of the product. In other words, while the *form* of the rapid prototype may be the same as that of the product, the *functional behavior* is, in general, different. In order to overcome this limitation, similitude techniques can be used to correlate the behavior of the prototype with that of the product. The two similitude techniques that are considered here include the traditional similitude method (TSM), which is also known as dimensional analysis, and the empirical similitude method (ESM).

II. Background

The TSM is a similitude method that relies solely on dimensional information to correlate the behavior of two similar systems. The ESM uses empirical data to correlate the behavior of two systems. Both the TSM and the ESM are reviewed briefly in the following sections.

2.1 Traditional Similarity Method, TSM

The field of dimensional analysis (herein referred to as the TSM) has developed over several centuries. The basic idea of the TSM is to create scale factors, based on the dimensions of system parameters, which can be used to correlate the behavior of two similar systems. The first step in the TSM process is to recast the dimensional equation that describes the system into dimensionless form, as follows:

$$g(d_1, d_2, \dots, d_n) = 0 \Rightarrow f(\pi_1, \pi_2, \dots, \pi_N) = 0 \quad (1)$$

where d_j , are dimensional parameters, π_i are dimensionless products, and $N < n$. For two similar systems (a product, p , and a model, m) the dimensionless products can be represented as

$$\begin{aligned} f(\pi_{p,1}, \pi_{p,2}, \dots, \pi_{p,N}) &= 0 \\ f(\pi_{m,1}, \pi_{m,2}, \dots, \pi_{m,N}) &= 0 \end{aligned} \quad (2)$$

or, in terms of a particular parameter of interest, say X , as

$$\begin{aligned} \pi_{p,X} &= f(\pi_{p,1}, \pi_{p,2}, \dots, \pi_{p,N-1}) \\ \pi_{m,X} &= f(\pi_{m,1}, \pi_{m,2}, \dots, \pi_{m,N-1}) \end{aligned} \quad (3)$$

For these two corresponding systems, the TSM states that $\pi_{p,X} = \pi_{m,X}$ if $\pi_{p,i} = \pi_{m,i}$ for all $i = 1, 2, \dots, N-1$. (Many references exist which show systematic derivations of dimensionless parameters from sets of dimensional parameters. See for example Barr, 1979 or Langhaar, 1951.)

Two systems which satisfy the TSM constraints ($\pi_{p,i} = \pi_{m,i}$ for all $i = 1, 2, \dots, N-1$) are said to be *well-scaled*, while systems which do not satisfy the constraints are said to be *distorted*. Many sources of system distortion exist which can produce errors in the TSM approach. If, for example, one of the dimensionless products contains a parameter that is constant in the model system but variable in the product system, then the system becomes distorted and the TSM yields inaccurate results.

2.2. Empirical Similarity Method, ESM

The empirical similarity method provides a means of correlating distorted systems. The fundamental concept of the ESM is shown in Figure 2. Unlike the traditional method, which relies solely on dimensional information for correlating systems, the ESM is able to correlate distorted systems by utilizing empirical data from a simplified specimen pair. The model specimen (ms) is a geometrically simplified version of the model, while the product specimen (ps) is a geometrically simplified version of the product. The ESM uses measured values from the model specimen, the product specimen, and the model to predict the behavior of the product. The basic assumptions of the ESM are as follows:

1. The model and the model specimen can be tested to determine the state variation caused by pure geometric changes (G).

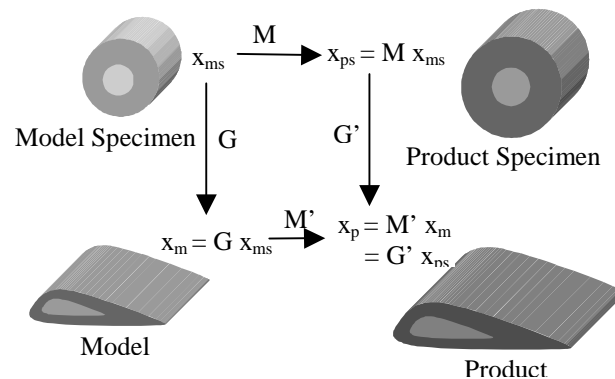


Figure 2. Empirical Similarity Method. Adapted from (Cho, 1999).

2. The model specimen and the product specimen can be tested to determine the state variation caused by pure non-geometric (material and loads) changes (M). The state of the product can be predicted by multiplying the state of the model by M' or by multiplying the state of the product specimen by G' , as shown in Figure 2. A basic assumption of the ESM is that $M = M'$ and $G = G'$ (Wood, 2002), or that M and G are *independent*.

Figure 3 shows qualitatively the applicability of ESM with respect to the TSM and direct product testing. We claim the ESM is a more accurate approach, in general, than the TSM. We also claim the ESM is a better approach for correlating systems with complex geometry whose governing parameters may not be well known, as required by the TSM. However, the range of application of the ESM, which is represented by the boundary lines in Figure 3, has not yet been clearly established. An evaluation of the current ESM boundaries, as well as a means to extend those boundaries, follows.

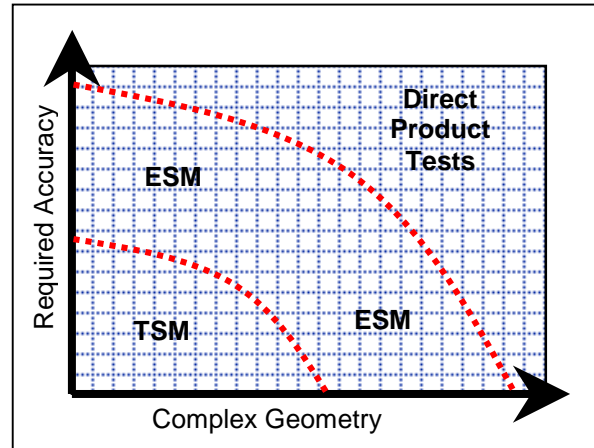


Figure 3. ESM vs. TSM

III. Evaluation of the Empirical Similitude Method

The ESM theory is valid as long as $M = M'$ and $G = G'$, as shown in Figure 2. Conditions that can cause $M \neq M'$ and $G \neq G'$, which are termed *specimen distortions*, are summarized in Figure 4. If the ESM can be set up with consistent scaling and with consistent material properties

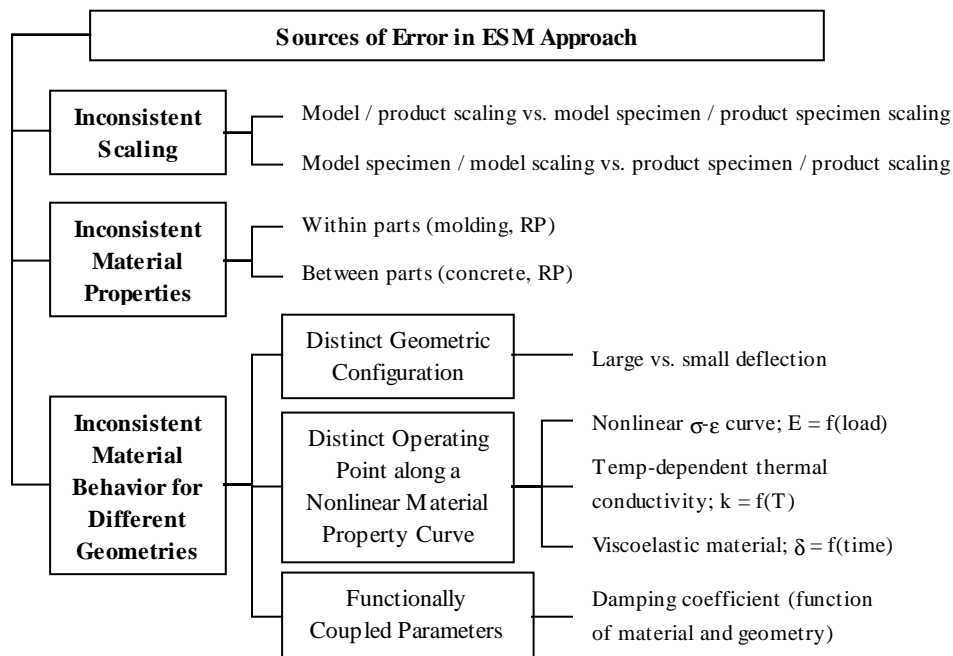


Figure 4. Sources of Error in the ESM.

in the model and product families, then the only source of specimen distortion will come from inconsistent material behavior in the model or product family. It is important to notice the subtle distinction that is made between material properties and material behavior: *material properties* refer to the global properties of the material; *material behavior* refers to the response of the material under some specific loading condition. For example a stress-softening material will behave differently – either “flexibly” or “stiffly” – depending on its specific operating point along the nonlinear stress-strain curve.

The ESM error that results from inconsistent material behavior is perhaps more subtle and difficult to anticipate than the other classes of specimen distortion. Three finite element studies are used to illustrate this type of specimen distortion. Each study illustrates one of the three subclasses of material behavior distortion that are listed in Figure 4. All three studies involve the deflection of a cantilever beam under an applied load at the tip. Each study involves some type of distortion between the model and the product (otherwise the TSM would be used rather than the ESM).

The product to be evaluated is a cantilever beam with five holes along the length. The ESM setup is shown in Figure 5. In each study, three different hole diameters are considered for the product beam (small holes with 0.15” diameter, medium holes with 0.25” diameter, and large holes with 0.35” diameter). Each beam is modeled with linear shell elements (S4R elements) using ABAQUS software. Large deflection effects are considered in each study. Beam deflection is monitored and recorded at ten equally spaced load increments.

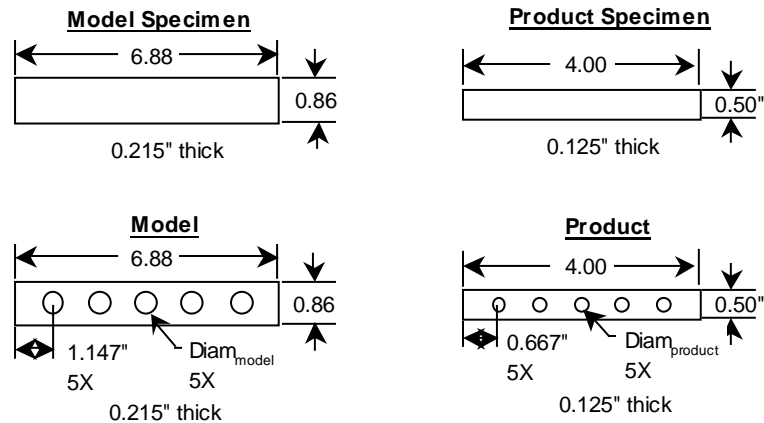


Figure 5. ESM Setup for Finite Element Studies.

3.1. ESM Study 1: Linear vs. Nonlinear Material Properties

The first ESM study involves a linear stress-strain curve for the product family and a nonlinear stress-strain curve for the model family. The constant value of Young’s modulus for the product family is 10,150 ksi (equal to that of aluminum). The variable value of Young’s modulus for the model family is defined with a Ramberg-Osgood curve, which is described by the following equation (see ABAQUS, 2001):

$$\varepsilon = \frac{\sigma}{E} \left(1 + \alpha \left(\frac{\sigma}{\sigma^0} \right)^{n-1} \right) \quad (4)$$

where σ = stress, ε = strain, E = Young’s modulus (defined as the slope of the stress-strain curve at zero stress), α = “yield” offset, σ^0 = yield stress, and n = hardening exponent for the “plastic” (nonlinear) term. By using different parameter values in equation 4, three different sets of

material properties with increasing degrees of nonlinearity were defined (see Table 1). Evaluating three geometric cases for each of the three different material properties gives a total of nine cases for this study. In each case, the ESM prediction of beam deflection is compared to the actual beam deflection, and a percent error in the ESM prediction is calculated. A plot of the results is shown in Figure 6 (note that the degree of model distortion corresponds to the material number). The error at “0” model distortion, which corresponds to a well-scaled system, is assumed to be zero.

Table 1. Parameters for Ramberg-Osgood Curve.

	E (ksi)	α	σ^0 (ksi)	n
Material 1	150	0.40	3	2.0
Material 2	320	0.43	3	3.0
Material 3	500	2.00	3	2.5

Because the model material has a nonlinear stress-strain curve, a change in geometry produces a different effect in the model family than it does in the product family. This source of ESM error can be understood more clearly by plotting the maximum stress for the various geometric configurations. Figure 7 contains such a plot for material 2. Notice that as the holes get bigger, the maximum stress (which occurs at the stress concentration around the first hole) increases. As the maximum stress increases, the model material behaves in a more flexible manner (i.e. the effective value of Young’s modulus decreases) while the product material remains the same (with a constant value of Young’s modulus). Since the material behavior is dependent on geometry, the ESM assumption is violated and errors result.

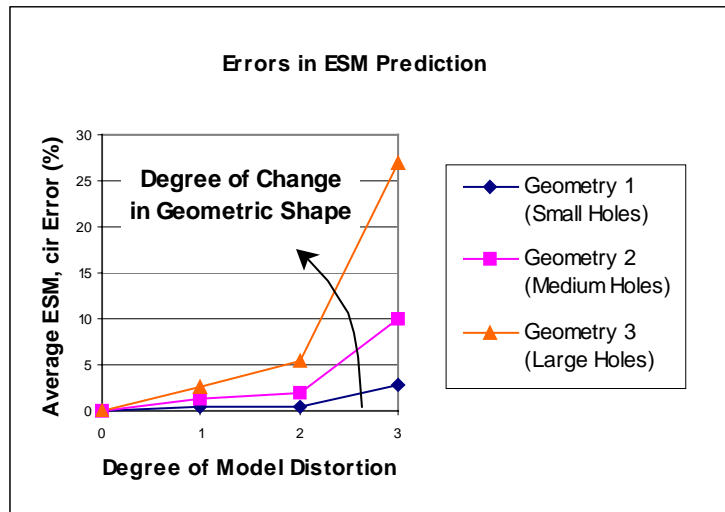


Figure 6. Results for ESM Study 1.

3.3. ESM Study 2: Parameter Distortion

The second ESM study investigates the effect of distorting the *length* of the model and the model specimen. All of the other beam parameters are well scaled. The five beam lengths that are considered are shown in Table 2. Note that the second length shown (6.88”) corresponds to a well-scaled system, and we would expect no error in either the TSM or the

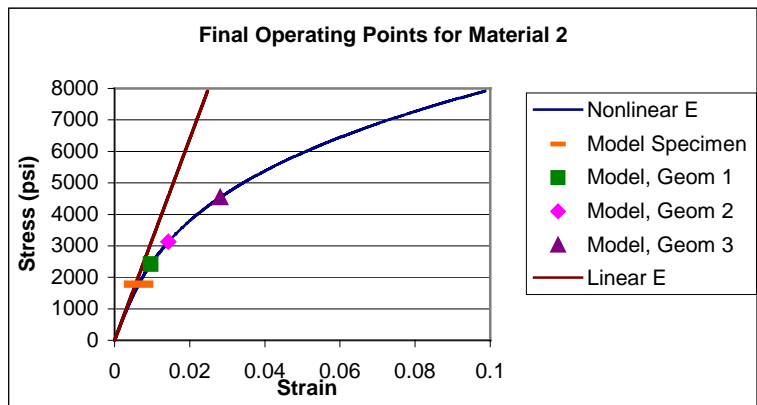


Figure 7. Maximum Stress for Various Geometries.

Table 2. Beam Lengths.

	Length (in)
Length 1	4.00
Length 2	6.88
Length 3	8.00
Length 4	12.0
Length 5	16.0

ESM results. The first length value represents a model beam that is “too short,” and the last three length values represent model beams that are “too long.” The results of the study are shown in Figure 8.

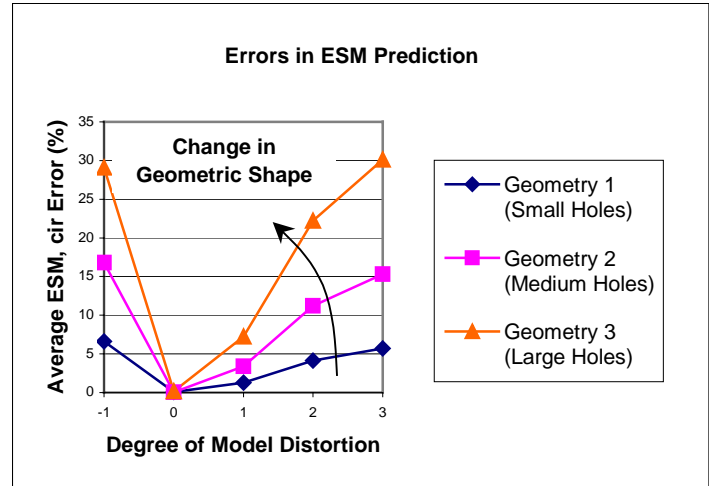


Figure 8. Results for ESM Study 2.

The ESM error is caused by the fact that the length distortion in the model family produces a different *geometric configuration* in the model family than in the product family. Because of large deflection effects, a change in geometry in the product yields a different change in beam deflection than a corresponding change in the geometry of the (already highly deflected) model.

3.3. ESM Study 3: Isotropic vs. Orthotropic Material Properties

The final ESM study involves isotropic material properties in the product family and orthotropic material properties in the model family. Both the tensile modulus and the shear modulus in the z-direction (out of the page in Figure 5) of the beam were distorted. Since deflection due to shear is dependent on both the shear modulus and the beam geometry, the ESM assumption is violated, and errors result. Results of this study are shown Figure 9.

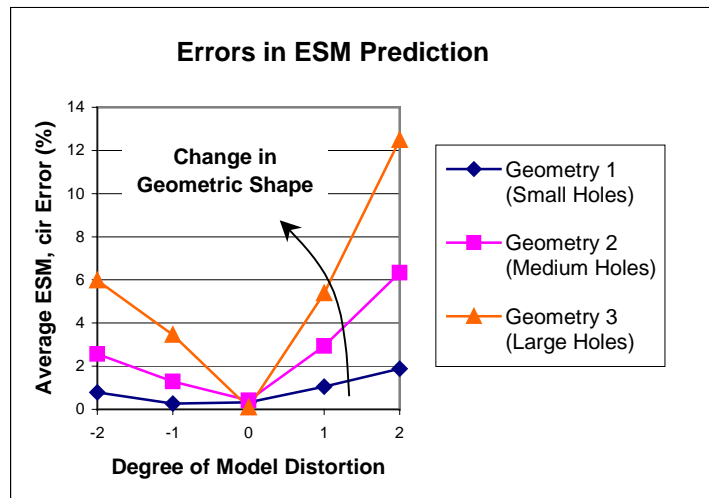


Figure 9. Results of ESM Study 3.

IV. Modified ESM Approach

The three studies presented above illustrate situations in which the ESM assumptions are no longer valid and $M \neq M'$ and $G \neq G'$. The modified ESM approach captures the change in the M transformation matrix as the geometry changes by utilizing

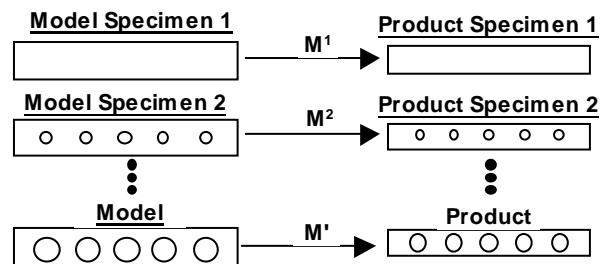


Figure 10. Modified ESM Approach.

one or more specimen pairs (see Figure 10). By quantifying the change in M with respect to the change in hole diameter, a Newton interpolating polynomial can be constructed to predict M' . Of course, the more intermediate specimens that are used, the higher the degree of the interpolating polynomial will be and the higher the prediction accuracy of M' will be. Figure 11 shows the improvement in ESM prediction accuracy for the “large holes” case of Study 1 using both 1st order and 2nd order polynomials. Similar improvements in prediction accuracy were also realized in studies 2 and 3.

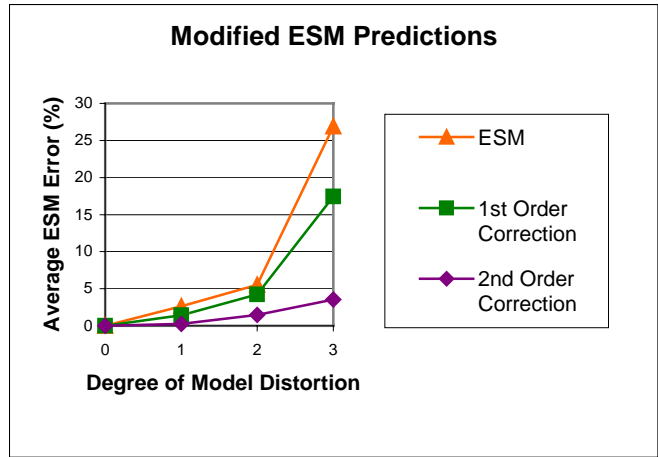


Figure 11. Modified ESM Results for Study 1.

V. Conclusions

The ESM has shown significant improvements over the TSM in predicting product performance when distortions between the product and the model exist. While the ESM typically produces highly accurate results, several sources of specimen distortion, which cause the ESM assumptions to become invalid, have been identified. The studies presented in this paper illustrate the ESM prediction error that can result from various types of specimen distortion. A modified ESM approach, which uses intermediate specimen pairs to capture the change in the transformation matrix as the geometry changes, has been shown to improve ESM predictions.

Further areas of research include expanding the results presented here into other areas, such as heat transfer applications. In addition, further research is needed to be able to quantify the change in the transformation matrix when the geometry change involves different geometric shapes. Finally, an overall approach for functional testing with rapid prototypes is needed which indicates which method (TSM, ESM, modified ESM, or direct product testing) is appropriate for different situations.

References

- ABAQUS/Standard User’s Manual, version 6.2. 2001. Hibbitt, Karlsson & Sorensen, Inc.
- Barr, D. I. H. 1979. “Echelon Matrices in Dimensional Analysis,” *International Journal of Mechanical Engineering Education*, Vol. 7, No. 2, pp. 85-89.
- Cho, U., Wood, K. L., and Crawford, R. H. 1999. “System-Level Functional Testing for Scaled Prototypes with Configurational Distortions,” *Proceedings of the 1999 ASME DETC*, Las Vegas, NV, ASME.
- Langhaar, H. L. 1951. *Dimensional Analysis and Theory of Models*, John Wiley & Sons, New York.
- Wood, J. J., Wood, K. L., and Troxell, W. O. 2002. “Empirical Analysis Using Advanced Similarity Methods,” to appear in *Proceedings of the 2002 ASME DETC*, Montreal, CA, ASME.